

# Dielectric Liquid Microlens With Switchable Negative and Positive Optical Power

Su Xu, Hongwen Ren, Yifan Liu, and Shin-Tson Wu, *Fellow, IEEE*

**Abstract**—We propose an adaptive dielectric liquid microlens whose focal length can be tuned from negative to positive or vice versa. The biconcave polymer base in the lens cell not only generates an inhomogeneous electric field, inhibits drifting of the droplet, and reduces the operating voltage but also induces a negative optical power. Pairing with the top subliquid lens, the whole lens exhibits a tunable negative and positive optical power under different driving voltages. To prove this concept, we fabricated such a dielectric liquid microlens and evaluated its performance. The biconcave polymer base can be particularly designed to obtain different dynamic range as desired. [2010-0226]

**Index Terms**—Adaptive optics, dielectric liquid, polymer, tunable lens.

## I. INTRODUCTION

**E**LECTROWETTING and dielectrophoretic (dielectric) effects are two most attractive approaches for adaptive liquid lenses because of their high optical performances and voltage switchable focal lengths [1]–[10]. Different from an electrowetting lens which uses oil and salty water, the two liquids employed in a dielectric lens are nonconductive. Therefore, the dielectric lens can bear a high operating voltage while keeping low power consumption. The latter is particularly important because it prevents microbubbles and liquid evaporation from happening during voltage actuation. In a conventional dielectric lens cell, the two immiscible liquids have different dielectric constants: one liquid forms a droplet on the bottom substrate, and the other liquid fills the surrounding space. Under the influence of an inhomogeneous electric field, the droplet surface is reshaped by the generated dielectric force, and the focal length is tuned accordingly. However, the previously demonstrated dielectric lenses are either positive or negative [1]–[4] so that the range of focal length change is relatively narrow. It would be highly desirable to have a dielectric liquid lens whose focal length can be tuned from positive to negative or vice versa. Such an adaptive lens can be integrated into a

Manuscript received July 27, 2010; revised October 3, 2010; accepted November 11, 2010. Date of publication January 14, 2011; date of current version February 2, 2011. This work was supported in part by the Air Force Office of Scientific Research under Contract FA95550-09-1-0170. Subject Editor J. A. Yeh.

S. Xu, Y. Liu, and S.-T. Wu are with the College of Optics and Photonics, University of Central Florida, Orlando, FL 32816 USA (e-mail: suxu@creol.ucf.edu; liufy423@knights.ucf.edu; swu@mail.ucf.edu).

H. Ren is with the Department of Polymer Nano-Science and Engineering, Chonbuk National University, Chonju 561-756, Korea (e-mail: hongwen@jbnu.ac.kr).

Color versions of one or more of the figures in this paper are available online at <http://ieeexplore.ieee.org>.

Digital Object Identifier 10.1109/JMEMS.2010.2100032

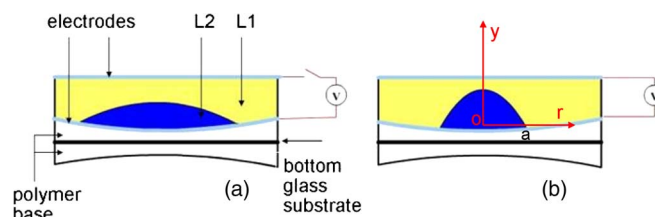


Fig. 1. Side-view structure of the lens cell. (a) Voltage OFF. (b) Voltage ON.

TABLE I  
PROPERTIES OF LIQUID-1, LIQUID-2, POLYMER BASE,  
AND GLASS SUBSTRATE

	Dielectric Constant	Refractive Index	Density (g/cm <sup>3</sup> )	Color
Liquid-1	42	1.47	1.26	Clear
Liquid-2	4.7	1.67	1.25	Clear
Polymer Base	4.0	1.56	1.2	Clear
Glass Substrate	NA	1.53	NA	Clear

zoom lens system for obtaining large magnification or in a 2D–3D switchable display [11].

In this paper, we report a new dielectric liquid microlens with a biconcave polymer base. Such a structure helps to fix the position of microlens and reduce the operating voltage, as compared to a dielectric liquid microlens with common planar electrodes. The advantage of our lens is that it exhibits a switchable positive–negative optical power with an external voltage. The measured response time is  $\sim 15$  ms.

## II. DEVICE STRUCTURE AND WORKING PRINCIPLE

Fig. 1 shows the side-view structure of the proposed microlens cell. From top to bottom, it consists of a planar glass substrate with indium tin oxide (ITO) electrode, liquid-1 (Glycerol), liquid-2 (Optical Fluids SL-5267, from Santovac<sup>®</sup> Fluids), a bi-concave polymer base (Norland Optical Adhesive 81) with gold and palladium electrode on the top surface, and a bottom glass substrate. Liquid-2 with a low dielectric constant forms a biconvex droplet on the top surface of the polymer base, while liquid-1 with a high dielectric constant fills the surrounding space. These two liquids are so chosen because of their well-matched density for minimizing the gravity effect. Table I lists the properties of the two employed liquids, polymer base, and glass substrate.

In the relaxed state, the curvature of the droplet is minimal.

However, in a voltage ON-state, the biconvex liquid droplet will induce an inhomogeneous electric field. According to the

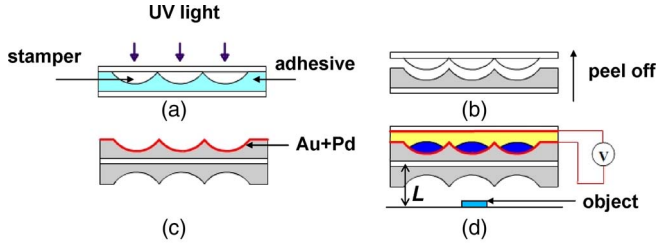


Fig. 2. Side view of the device fabrication procedure. (a) UV exposure. (b) Peeling off the stamper. (c) Making two sets of the polymer base and aligning them under a microscope, then coating Au + Pd electrode. (d) Dropping liquids and sealing the cell.

Kelvin theory, the dielectric force exerted on the droplet can be expressed as [12]

$$\vec{F} = \frac{\varepsilon_0}{2}(\varepsilon_1 - \varepsilon_2)\nabla(E \cdot E) \quad (1)$$

where  $\varepsilon_0$ ,  $\varepsilon_1$ , and  $\varepsilon_2$  donate the permittivity of free space, liquid-1, and liquid-2, respectively, and  $E$  is the electric field on the curved droplet surface. If the dielectric force is strong enough, liquid-1 and liquid-2 will move toward the region with strong and weak electric fields, respectively. The droplet tends to contract, and its surface profile is reshaped, resulting in a different focal length, as Fig. 1(b) shows. Due to the stronger electric field which originates from the closer electrode gap and larger affected droplet surface, the dielectric liquid lens with a well-shaped electrode has a lower operating voltage than that of the lens with common planar electrodes [4].

Because of the surface tension force of the droplet liquid, the shape of the droplet is curved, and its surface is very smooth. Like a deformed elastic membrane [13], if we consider the surface of the droplet as a very thin elastic membrane, then the shape of the droplet can be expressed by

$$y = \frac{1}{2}(P/2S)(a^2 - r^2) + \frac{1}{16}(P/2S)^3(a^4 - r^4) + \dots \quad (2)$$

Here,  $y$  is the vertical axis, and  $r$  is the horizontal axis passing through the droplet center, as shown in Fig. 1(b). At  $y = 0$ ,  $r = a$  (the radius of droplet aperture). The droplet experiences a surface tension force  $S$  and a pressure force  $P$ . When the droplet radius is small, we can neglect the higher order terms in (2) and only keep the first item, which implies that the droplet presents a parabolic shape. When the droplet is activated, the external voltage causes the pressure force  $P$  to increase which, in turn, changes the droplet's shape. However, the droplet keeps a parabolic shape.

### III. FABRICATION PROCESS

Fig. 2 shows the device fabrication procedures. In Fig. 2(a), a small amount of adhesive was injected into a glass cell. The cell was composed of a glass substrate and a glass-based plano-convex microlens array ( $R = 1$  mm,  $\varnothing = 0.75$  mm,  $6 \times 6$ , and from Isuzu Glass), which was adopted as a stamper. After UV curing, the stamper was peeled off, and the solidified concave microlens pattern was left on the bottom glass substrate [Fig. 2(b)].

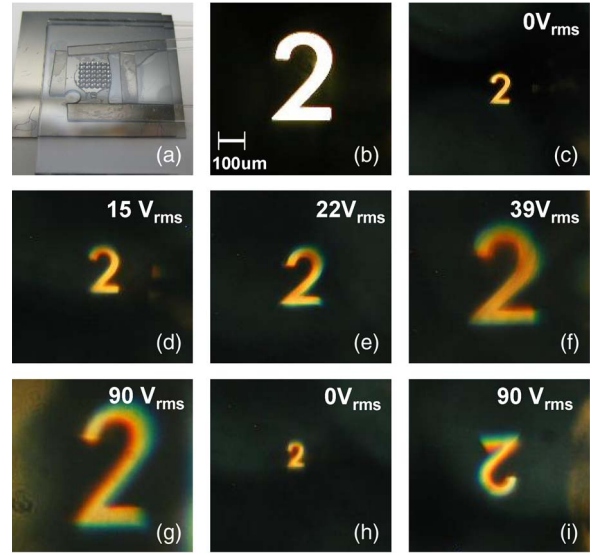


Fig. 3. (a) Top view of the device. The image observed through the microscope at  $L = 3$  mm (b) without any liquid lens, and (c)–(g) with the dielectric liquid microlens driven at different voltages, and at  $L = 7$  mm. (h)  $V = 0$ , and (i)  $V = 90 V_{rms}$ .

Two sets of microlens pattern were fabricated and were carefully aligned under the microscope to form a biconcave polymer base. To prove this concept, we deposited a conducting layer (alloy of gold and palladium) by using a sputter coater (from EMITECH) on the top surface of the base as the bottom electrode, as shown in Fig. 2(c). Finally, after dropping liquid-2 and liquid-1, a planar glass with ITO was used as top substrate, and the cell was sealed, as Fig. 2(d) shows, and a top view of the lens cell is shown in Fig. 2(a). The cell gap is  $\sim 270 \mu\text{m}$ .

### IV. RESULTS AND DISCUSSION

The performance of the dielectric liquid microlens with a biconcave polymer base was evaluated through an optical microscope. A small number “2” as an object was placed under the microscope. First, the distance between the object and the bottom glass substrate  $L$ , as shown in Fig. 2(d), was set at 3 mm. Fig. 3(b) shows the image observed through the microscope without any dielectric liquid microlens. Then, we inserted the liquid lens in the optical path, refocused the microscope, and observed the images again. A virtual erect and diminished image was observed at  $V = 0$  [Fig. 3(c)], which indicated that our lens showed a negative optical power. The image began to grow when actuated at  $15 V_{rms}$  and kept growing as the voltage was further increased. This is because the droplet of liquid-2 gradually contracts as the driving voltage increases, leading to a reshaped droplet profile. As a result, the optical power of the top sublens (the positive liquid lens consisting of liquid-1 and liquid-2) is enhanced, while that of the lower sublens (the biconcave polymer base) is kept constantly negative, thus the optical power of the entire liquid lens goes less negative, and the virtual erect image is magnified gradually, as shown in Fig. 3(d) and (e). At  $V = 39 V_{rms}$ , the image size [Fig. 3(f)] was almost the same as that of the original image [Fig. 3(b)]. This implies that the optical power of the top and the lower sublenses are cancelled with each other, and the whole lens

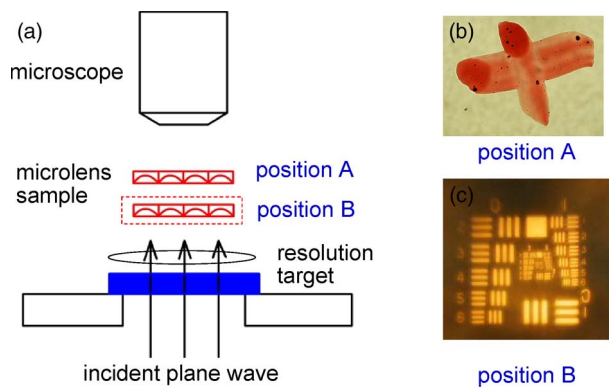


Fig. 4. (a) Experimental setup for measuring the focal length. (b) Focusing on the top glass substrate. (c) Focusing on the image of the target.

shows no optical power. At  $V = 90 V_{\text{rms}}$ , the image [Fig. 3(g)] is still erect, but the size is larger than that of the original image. Further contraction in the droplet eventually turns the whole lens into a positive optical power. In another experiment, we increased the distance between the target and the bottom glass substrate  $L$  to 7 mm. At  $V = 0$ , the size of the erect image [Fig. 3(h)] was further reduced as compared to that in Fig. 3(c) because the distance between the object and the liquid lens was increased. At  $V = 90 V_{\text{rms}}$ , an upside down and diminished image [Fig. 3(i)] was observed. These indicate that the focal length of our liquid lens is electrically tunable, and its optical power can be continuously tuned between negative and positive.

Chromatic aberration is observed in the images due to material dispersion. The Abbe number of liquid-2 is relatively small at  $\sim 22$ . Meanwhile, the curvature of the droplet increases with the operating voltage. As a result, the chromatic aberration is severe in the high-voltage state [14]. To reduce chromatic aberration, we need to choose proper liquids with a large Abbe number.

A small scattering is also observed due to slight nonuniformity of the well-shaped electrode, which originates from the slow stage rotation speed of the sputter coater. Coaxial design is important in order to maintain good optical functions of a liquid lens [15]. The optic axis of our liquid lens is slightly deviated from its normal because of the minor misalignment in the biconcave polymer base and the nonuniformity of the bottom well-shaped electrode. The transmittance of our lens is  $\sim 50\%$  at  $\lambda = 550 \text{ nm}$ . Most of the loss originates from the absorption of the metal electrode (Au-Pd alloy) and from interface reflections. These drawbacks can be overcome by coating the ITO electrode on a commercial biconcave microlens and applying specific liquid confinement structures [15].

The back focal distance (BFD) of the dielectric microlens shown earlier was measured through a microscope. Fig. 4 shows the experimental setup for the measurement. A resolution target placed directly above the lamp was used as an object for imaging, and the lens sample was placed on the stage of the microscope. A “red cross” was marked on the top glass substrate for focusing. At first, we adjusted the stage until seeing a clear image of the “red cross,” and the position of the stage was marked as position A, as shown in Fig. 4(b). Then, we adjusted the stage to get a clear image of the target bar, and the position of the stage was marked as position B [Fig. 4(c)].

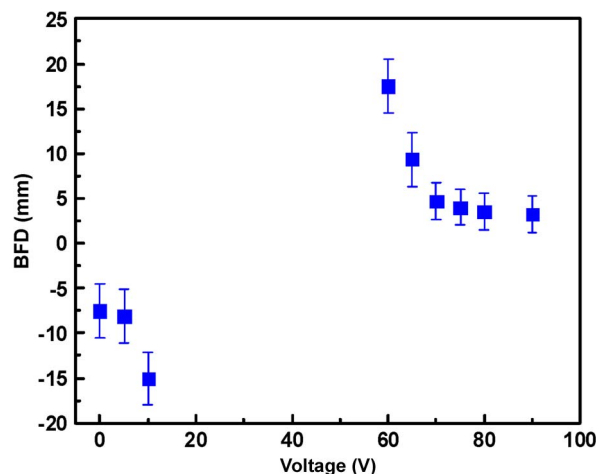


Fig. 5. Measured focal length of the dielectric liquid microlens at different driving voltages.

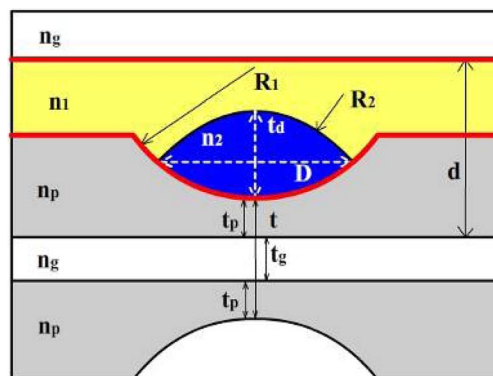


Fig. 6. Lens structure and parameters for Zemax simulation.

Comparing the focal length with the object distance, the position of the object can be assumed as infinity. Thus, the distance from position A to B is considered as BFD of the dielectric liquid microlens. The voltage dependent focal length is shown in Fig. 5 as blue dots. At  $V = 0$ , the inherent focal length of the microlens is  $\sim -7.56 \text{ mm}$ . As the voltage increases, the focal length first goes to negative infinity at  $V \sim 39 V_{\text{rms}}$ , and then comes in from positive infinity. At  $V = 90 V_{\text{rms}}$ , it is decreased to  $\sim 3.22 \text{ mm}$ .

We also calculate the theoretical BFD in Zemax. The lens structure and parameters used for Zemax simulation are shown in Fig. 6, where  $n_1$ ,  $n_2$ ,  $n_g$ , and  $n_p$  donate the refractive index of liquid-1, liquid-2, glass substrate, and polymer base, respectively.  $D \sim 0.72 \text{ mm}$  is the initial aperture of the lens;  $d \sim 0.27 \text{ mm}$  is the cell gap of the lens cell.  $t_g \sim 0.42 \text{ mm}$  is the thickness of the bottom glass substrate,  $t_p \sim 0.032 \text{ mm}$  is the apex distance of one plano-concave polymer base, and  $t$  is that of the biconcave polymer base ( $\sim 2t_p + t_g$ ).  $R_1$  is the curvature radius of the polymer base, which is equal to that of the plano-convex microlens array stamper, because this base is replicated from the stamper.  $R_2$  is the curvature radius of the top surface of the droplet, and  $t_d$  is the apex distance of the droplet. The top surface of the droplet is considered as parabolic shape in the Zemax simulation. Both  $R_2$  and  $t$  vary with the operating voltage. All of these parameters affect the dynamic range of the lens. If  $R_1$  is changed, the profile of the droplet at the relaxed

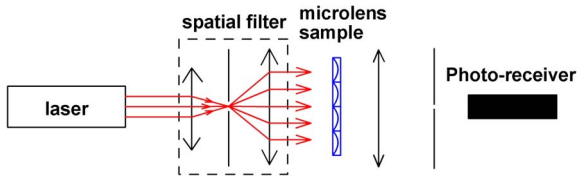


Fig. 7. Experimental setup for measuring the response time.

state and actuated state will be changed accordingly, leading to a varied dynamic range. Therefore, we may particularly design  $R_1$  to provide the dynamic range as required. In the relaxed state, the measured apex distance is  $t_d \sim 0.147$  mm, and the calculated BFD is  $\sim -9.0$  mm, while the measured BFD is  $\sim -7.56$  mm. At  $V = 90 V_{\text{rms}}$ , the measured  $D$  and  $t_d$  are  $\sim 0.606$  mm and  $\sim 0.167$  mm, respectively. The calculated BFD is  $\sim 2.49$  mm, which is slightly shorter than the measured data ( $\sim 3.22$  mm) at  $V = 90 V_{\text{rms}}$ . These minor differences are attributed to the assumption of infinity object and the measurement error of lens dimension because it is difficult to precisely measure the dimension of such a small liquid droplet through an optical microscope.

Response time is another important issue for adaptive liquid lenses. In a dielectric liquid lens, the contracting speed of the droplet mainly depends on the dielectric force, and the relaxing speed depends on the viscosity of the liquids and the related interfacial tensions [3]. Since the deformation of a liquid droplet profile is related to the balance of electric energy, surface energy, adhesion energy, and gravitational energy [1], it is very difficult to theoretically calculate the response time. Thus, we measured the lens response time using the setup shown in Fig. 7. The lens sample was mounted on a linear metric stage. A He-Ne ( $\lambda \sim 633$  nm) laser beam was collimated and expanded to illuminate the sample. A large area visible photoreceiver (Model 2031, New Focus) connected to an oscilloscope (TDS 3032B, Tektronix) was used to measure the intensity variation induced by the dielectric liquid microlens. We applied a square voltage of  $90 V_{\text{rms}}$  ( $f \sim 300$  Hz) to the lens cell. The contracting and the relaxing speeds were measured to be  $\sim 13$  ms and  $\sim 18$  ms, respectively.

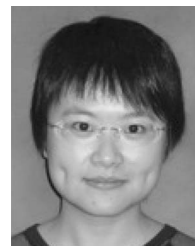
## V. CONCLUSION

We have reported a dielectric liquid microlens with tunable positive and negative optical power. The negative optical power induced by the biconcave polymer base balances out the positive optical power of the liquid droplet to some extent, according to different operating voltage. Thus, our lens can be continuously tuned among negative, zero, and positive optical power states. Moreover, the biconcave polymer base helps to fix the position of the liquid droplet and reduce the operating voltage. The focal length can be tuned from  $\sim -7.56$  mm to infinity to  $\sim 3.22$  mm when the voltage increases from 0 to  $90 V_{\text{rms}}$ . The response time is reasonably fast:  $\sim 13$  ms in rising and  $\sim 18$  ms in relaxing. The transmittance, scattering, and the deviation of the optical axis in the lens can be improved by coating ITO on a commercial biconcave microlens. The dimension of the biconcave polymer base can be particularly designed to get the desired lens' dynamic range. Our approach has enabled

focus tuning from negative to positive or vice versa in a single dielectric lens without any moving part. Such a liquid microlens will find potential applications in vision and imaging devices.

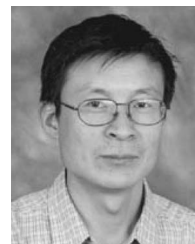
## REFERENCES

- [1] C. C. Cheng and J. A. Yeh, "Dielectrically actuated liquid lens," *Opt. Express*, vol. 15, no. 12, pp. 7140–7145, May 2007.
- [2] H. Ren and S. T. Wu, "Tunable-focus liquid microlens array using dielectrophoretic effect," *Opt. Express*, vol. 16, no. 4, pp. 2646–2652, Feb. 2008.
- [3] H. Ren, H. Xianyu, S. Xu, and S. T. Wu, "Adaptive dielectric liquid lens," *Opt. Express*, vol. 16, no. 9, pp. 14954–14960, Sep. 2008.
- [4] S. Xu, Y. J. Lin, and S. T. Wu, "Dielectric liquid microlens with well-shaped electrode," *Opt. Express*, vol. 17, no. 13, pp. 10499–10505, Jun. 2009.
- [5] H. Ren, Y. H. Lin, and S. T. Wu, "Adaptive lens using liquid crystal concentration redistribution," *Appl. Phys. Lett.*, vol. 88, no. 19, pp. 191116-1–191116-3, May 2006.
- [6] Y. J. Lin, K. M. Chen, and S. T. Wu, "Broadband and polarization-independent beam steering using dielectrophoresis-tilted prism," *Opt. Express*, vol. 17, no. 10, pp. 8651–8656, May 2009.
- [7] H. Ren, S. Xu, and S. T. Wu, "Deformable liquid droplets for optical beam control," *Opt. Express*, vol. 18, no. 11, pp. 11904–11910, May 2010.
- [8] C. G. Tsai and J. A. Yeh, "Circular dielectric liquid iris," *Opt. Lett.*, vol. 35, no. 14, pp. 2484–2486, Jul. 2010.
- [9] M. Vallet, B. Berge, and L. Volvelle, "Electrowetting of water and aqueous solutions on poly (ethylene terephthalate) insulating films," *Polymer*, vol. 37, no. 12, pp. 2465–2470, Jun. 1996.
- [10] H. Ren and S. T. Wu, "Optical switch using a deformable liquid droplet," *Opt. Lett.*, vol. 35, no. 22, pp. 3826–3828, Nov. 2010.
- [11] H. Choi, J. H. Park, J. Kim, S. W. Cho, and B. Lee, "Wide-viewing-angle 3D/2D convertible display system using two display devices and a lens array," *Opt. Express*, vol. 13, no. 21, pp. 8424–8432, Oct. 2005.
- [12] J. D. Jackson, *Classical Electrodynamics*, 2nd ed. New York: Wiley, 1975.
- [13] G. C. Knollman, J. L. Bellin, and J. L. Weaver, "Variable-focus liquid-filled hydroacoustic lens," *J. Acoust. Soc. Amer.*, vol. 49, no. 1B, pp. 253–261, Jan. 1971.
- [14] P. Ruffieux, T. Scharf, H. P. Herzig, R. Völkel, and K. J. Weible, "On the chromatic aberration of microlenses," *Opt. Express*, vol. 14, no. 11, pp. 4687–4694, May 2006.
- [15] C. G. Tsai, C. N. Chen, L. S. Cheng, C. C. Cheng, J. T. Yang, and J. A. Yeh, "Planar liquid confinement for optical centering of dielectric liquid lenses," *IEEE Photon. Technol. Lett.*, vol. 21, no. 19, pp. 1396–1398, Oct. 2009.



**Su Xu** received the B.S. degree in information engineering and the M.S. degree in optical engineering from Zhejiang University, Hangzhou, China, in 2004 and 2006, respectively. She is currently working toward the Ph.D. degree in the College of Optics and Photonics, University of Central Florida, Orlando.

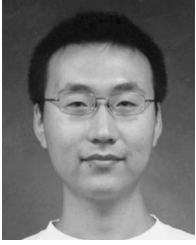
Since 2007, she has been a Research Assistant in the Photonics and Display Group, University of Central Florida. Her current research focuses on adaptive-focus liquid and liquid crystal lenses and other adaptive liquid devices.



**Hongwen Ren** received the Ph.D. degree from Changchun Institute of Optics, Chinese Academy of Sciences, Beijing, China.

He joined the College of Optics and Photonics, University of Central Florida, Orlando, as a Research Scientist in 2001. Since 2009, he has been an Assistant Professor in the Department of Polymer-Nano Science and Engineering, Chonbuk National University, Chonju, Korea. He has published over 40 journal papers, one book chapter, and is the holder of eight U.S. patents. His research concentrates on adaptive-focus lenses, variable optical attenuators, and tunable photonic devices.

focus lenses, variable optical attenuators, and tunable photonic devices.



**Yifan Liu** received the B.S. degree in electronic science and technology from Tsinghua University, Beijing, China, in 2007, and the M.S. degree in electrical and computer engineering from The Ohio State University, Columbus, in 2009. He is currently working toward the Ph.D. degree in optics at the University of Central Florida, Orlando.

Since 2009, he has been a Research Assistant in the Photonics and Display Group, University of Central Florida. His current research focuses on 3-D displays and adaptive liquid devices.

**Shin-Tson Wu** (F'04) received the Ph.D. degree in physics from the University of Southern California, Los Angeles.

He is a Pegasus Professor in the College of Optics and Photonics, University of Central Florida (UCF), Orlando. Prior to joining UCF in 2001, he was with Hughes Research Laboratories, Malibu, CA, for 18 years. He has coauthored six books, seven book chapters, over 360 journal papers, and 63 issued U.S. patents.

Prof. Wu is a Fellow of the Optical Society of America (OSA), Society of Photo-Optical Instrumentation Engineers, and Society for Information Display (SID). He was the recipient of the OSA Joseph Fraunhofer Award/Robert M. Burley Prize, SPIE G. G. Stokes Award, and SID Jan Rajchman Prize. He was the founding Editor-in-Chief of the IEEE/OSA JOURNAL OF DISPLAY TECHNOLOGY.